

Whole Liver Fat Quantification in Pediatric Patients with NonAlcoholic Fatty Liver Disease (NAFLD)

Xiaodong Zhong¹, Jie Deng^{2,3}, Brian M. Dale⁴, Cynthia K. Rigsby^{2,3}, and Mark H. Fishbein⁵

¹MR R&D Collaborations, Siemens Healthcare, Atlanta, GA, United States, ²Department of Medical Imaging, Ann & Robert H. Lurie Children's Hospital of Chicago, Chicago, IL, United States, ³Department of Radiology, Feinberg School of Medicine, Northwestern University, Chicago, IL, United States, ⁴MR R&D Collaborations, Siemens Healthcare, Cary, NC, United States, ⁵Division of Gastroenterology, Hepatology, and Nutrition, Ann & Robert H. Lurie Children's Hospital of Chicago, Chicago, IL, United States

Target Audience. Pediatric radiologists and abdominal MR radiologists.

Purpose. The rapid evaluation and quantification of hepatic fat deposition for pediatric patients is of growing interest, as non-alcoholic fatty liver disease (NAFLD) is the primary form of chronic liver disease among children (1). Liver biopsy is the gold standard in clinic, but is an invasive approach with possible sampling errors and complications. MRI methods based on chemical shift imaging have been demonstrated to be promising to quantify hepatic fat, and multiple studies have been performed in multiple sites for adult patients (2-4). Although directly applicable in theory, to our knowledge, few studies of hepatic fat quantification have been done in pediatric patients. Early pediatric studies were limited to a two- or three-point Dixon method known to have bias due to confounding factors, such as T_2^* decay of fat and water, T_1 bias, and multi-peak fat modeling (5,6). A recent study applied a more advanced multi-echo technique to overcome these confounds, based on fitting signals of multiple regions of interest (ROI), and was validated with a liver-fat phantom and against liver biopsy in vivo in pediatric patients (7). Proton density fat fraction (PDFF) mapping with whole liver volume coverage would be clinically preferred. The purpose of this study was to perform a preliminary evaluation for a fat quantification mapping technique (4) in pediatric patients, using the ROI fitting method (7) as a reference standard.

Methods. Both the ROI fitting method (7) and the mapping method (4) utilize a multi-fat-peak model and separate T_2^* decay of fat and water. The signal model equation was shown as below, where ρ_w and ρ_f are water and fat quantities, respectively; T_{2w}^* and T_{2f}^* are water and fat T_2^* values, respectively; N_f is the number of fat peaks and f_n is the chemical shift frequency corresponding to the n th fat peak.

$$S(TE) = \left| \rho_w e^{-TE/T_{2w}^*} + \rho_f e^{-TE/T_{2f}^*} \cdot \sum_{n=1}^{N_f} C_n e^{2i\pi f_n TE} \right|$$

The T_1 bias is reduced by setting a low flip angle. These two methods use different non-linear least squares fitting algorithm to fit the signal equation model, with different initialization values and implementations.

In accordance with protocols approved by the local IRB, in vivo liver imaging data were acquired in 12 pediatric subjects with suspected or identified NAFLD (10-17 years old) on a 1.5 T MRI system (MAGNETOM Aera, Siemens, Erlangen, Germany) after informed consent forms were obtained. For the ROI fitting method, a 2D GRE acquisition with 4 slices was performed, with the parameters of FOV = 360×270 mm², pixel size = 1.9 mm, TR = 120 ms, TE = 2.3, 4.6, 6.9, 9.2, 11.5 and 13.8 ms, flip angle = 10° . The acquisition time was 12 s for each slice. The images were saved and used as input of the ROI fitting method (7) to generate PDFF values for multiple representative ROI positions offline, including one ROI on the left lobe and two on the right lobe, avoiding large hepatic vessels (Fig 1). For the mapping method, a 3D GRE sequence was performed to cover the whole liver in a single breath-hold (4). Parameters included TR = 20 ms, flip angle = 10° , pixel size = 1.9 mm, slice thickness = 5 mm, iPAT = 2, first TE = 2.3 ms, and 6 echoes collected with $\Delta TE = 2.3$ ms, partitions = 16. The acquisition time was 16 s. PDFF maps were generated inline (4). The ROIs used in the ROI fitting method were manually registered on the PDFF maps of the mapping method by an experienced MR physicist with care. PDFF values in these ROIs on the PDFF maps were measured with the Siemens Syngo software on the scanner, and were then averaged. Linear regression, intraclass correlation coefficient, and Bland-Altman analysis were performed to evaluate the averaged PDFF values measured with the ROI fitting method and the mapping method.

Results. Example PDFF map from one pediatric patient is shown in Fig. 1, where the mean FP was 33%, 35.2% and 36.0% within the ROI positions, respectively. The PDFF values measured with the ROI fitting method on the same positions were 32.6%, 33.5% and 35.1%, respectively.

Good linear correlation was found among the PDFF results of the two methods within the averaged PDFF values for all the patients (Fig. 2A). Bland-Altman plot also demonstrated good agreement (Fig. 3B). Intraclass correlation coefficient was 0.992 (95% CI: 0.972 to 0.998).

Discussion and Conclusions. In this work, a fat quantification mapping technique with whole liver coverage was evaluated for fat quantification in pediatric patients. For the protocols and patients tested in this study, this mapping method produced similar liver fat quantification results to those measured with a previously validated ROI fitting method as a reference standard. Future studies are warranted to further evaluate this mapping method in pediatric patients with different reference standards such as spectroscopic methods and liver biopsy. This single breath-hold fat quantification mapping method can be easily adopted in routine clinical scanning, and may have great potential for efficiently evaluating the hepatic steatosis for obesity related liver diseases in pediatric patients.

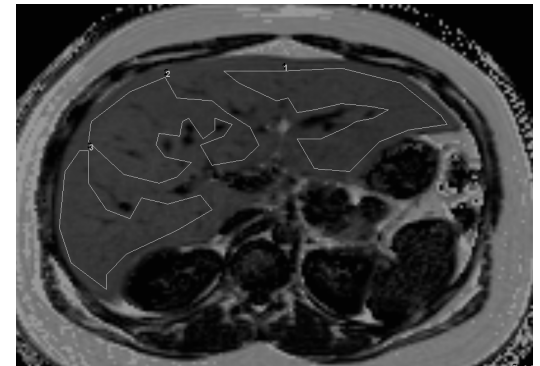


Fig. 1 Example PDFF map from one pediatric patient. One ROI on the left lobe and two ROIs on the right lobe were used in the ROI fitting method.

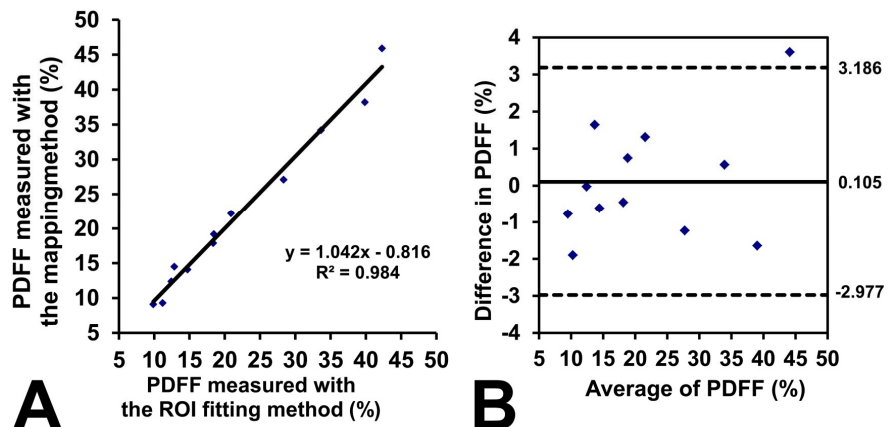


Fig. 2 Linear regression (A) and Bland-Altman analysis (B) between the PDFF results measured with the ROI fitting method and the mapping method.

1. Barshop et al. Aliment Pharmacol Ther 2008;28:13-24.
2. Hernando et al. Magn Reson Med 2010;63:79-90.
3. Bydder et al. Magn Reson Imaging 2008;26:347-359.
4. Zhong et al. Magn Reson Med 2014;72:1353-1365.
5. Kovanlikaya et al. Pediatric Radiology 2005;35:601-607.
6. Pacifico et al. World J Gastroenterol 2011; 17:3012-3019.
7. Deng et al. Pediatr Radiol 2014;44:1379-1387.